Research Article

Preparation and stability of astaxanthin solid lipid nanoparticles based on stearic acid

Miaomiao Li, Mohamed Reda Zahi, Qipeng Yuan, Feibao Tian and Hao Liang

State key Laboratory of Chemical Resource Engineering, Beijing University of Chemical Technology, Beijing, P. R. China

Astaxanthin (ASTA), a natural pigment carotenoid, is endowed with remarkable antioxidant activity in food and cosmetic products. However, the utilization of ASTA is limited due to its poor water-solubility, low bioavailability, and the decomposition under light, heat, and oxygen. In order to overcome these drawbacks, ASTA was encapsulated within solid lipid nanoparticles (SLNs). ASTA-SLNs, composed of lipid nucleation (ASTA, soybean oil, solid lipid matrix) and external water phase (Tween 20, deionized water), were prepared by high pressure homogenization (HPH). The contents of three different solid matrixes (stearic acid, glycerin monostearate, and glycerol distearates) and the preparation conditions (pressure and number of cycles) were optimized. Stearic acid (1 wt%) was selected on the basis of physico-chemical properties of ASTA-SLNs, such as mean particle size, zeta potential, and polydispersivity index (PDI). Moreover, ASTA-SLNs exhibited good long-term stability at 4 and 25°C, with no significant modification in the particle size. Comparative with the free ASTA, the chemical stability of ASTA in SLNs was significantly enhanced. Finally, the release experiments of ASTA-SLNs showed that SLNs could provide prolonged release of ASTA in simulated gastric and intestinal juices.

Practical application: SLNs, a promising submicron drug delivery system, could be widely applied in food, cosmetics, drugs, and health products. In the fields of targeted delivery and controlled release of drugs, SLNs have attracted increasing attention. ASTA-SLNs can be prepared into various pharmaceutical dosage forms, such as oral tablet, intravenous infusion, and percutaneous absorption, thus achieving a long-time and stable therapeutic effect in small dosage. More importantly, based on the high pressure homogenization technology, ASTA-SLNs can be produced in large-scale.

Keywords: Astaxanthin / Release / Solid lipid nanoparticles / Stability / Stearic acid

Received: December 18, 2014 / Revised: April 8, 2015 / Accepted: May 22, 2015

DOI: 10.1002/ejlt.201400650

1 Introduction

Astaxanthin (3,3′-dihydroxy-β-β′-4-4′-carotene-dione, ASTA), one of the natural carotenoid pigments, is found in aquatic organisms such as shrimp, shuck, and salmon [1, 2]. ASTA has many pharmacological activities which could reduce the risk of cancer, tumors, and cardiovascular diseases [3–5]. Its ability of exhibiting oxygen free radicals was superior to vitamin E, coenzyme Q_{10}, and β-carotenoid [6]. However, its bioaccessibility has suffered a significant challenge due to its low water solubility and poor chemical stability [7]. A highly unsaturated molecular structure makes ASTA susceptible to light, oxide, heat, alkaline, and acidic solution [8]. Therefore its application was limited in the food and medicine industries.

Microencapsulation technologies, such as inclusion complex, liposome, nanoparticles, and emulsion, have been widely used for protecting nutritional functional compounds against degradation [9, 10]. These technologies enhanced the physicochemical stability of hydrophilic and lipophilic ingredients through packaging them with wall materials [11]. The wall materials are crucial to the products performance and release behavior. In recent years, encapsulation of ASTA

Correspondence: Prof. Hao Liang, Department of Science and Technology of Life, State key Laboratory of Chemical Resource Engineering, Beijing University of Chemical Technology, P.O. Box 75, No. 15, Bei San Huan Dong Rd., Beijing, P. R. China
E-mail: lianghao@mail.buct.edu.cn
Fax: +86 10 64437610

Abbreviations: ASTA, astaxanthin; **GDS,** glycerol distearates; **GMS,** glycerol monostearate; **HPH,** high pressure homogenization; **PDI,** polydispersity index; **SA,** stearic acid; **SD,** standard deviation; **SLNs,** solid lipid nanoparticles; **Tween 20,** polysorbate 20; **Z-average,** average particle size

has been paid for great attention. Cyclodextrins and its derivatives, containing peculiar hydrophobic cavity, are often used to form inclusion complexes [12]. As reported by Yuan and co-workers, the inclusion complex of ASTA with hydroxypropyl-β-cylodextrin was prepared and characterized by FTIR and TG/DTA [13]. Thermal degradation of ASTA could also be prevented through encapsulation into polymeric nanospheres [14]. But high molecular weight polymers are not easily to be digested in human body, so it is essential to develop new delivery carrier for ASTA.

Solid lipid nanoparticles (SLNs), a novel submicron sized drug delivery system, offer a high innovative potential in pharmaceutical, cosmetic, and food applications [15]. This colloidal system possesses many brilliant properties, such as biocompatibility, non-toxicity, biodegradability, and physicochemical stability [16]. SLNs were composed of solid lipid matrix, vegetable oil, surfactant, and active ingredient [17]. The crystalline networks of solid lipid matrix in nucleation, prepared by precipitation of microemulsion, not only improve encapsulation efficiency of drugs, but also control the release behavior of drugs [18]. Natural or synthetic solid lipid matrixes are biocompatible and biodegradable, such as fatty acid, glycerine ester, and triglyceride [19, 20]. Therefore, SLNs have attracted increasing attention as suitable colloidal carriers for delivery of drugs with limited solubility. SLNs for tetracycline were successfully prepared and investigated the physicochemical characterization [21]. Additionally, SLNs were able of incorporating therapeutic peptides, proteins, and antigens to avoid proteolytic degradation [22]. However, there was no report about the formulation of ASTA solid lipid nanoparticles (ASTA-SLNs).

SLNs production has employed several technologies including microemulsions, solvent evaporation, solvent emulsification, film-ultrasound diffusion, high pressure homogenization (HPH) [23, 24]. Since HPH can avoid or significantly reduce chemical usage, it is a reliable technology for preparing SLNs by high shear stress and cavitation forces of high pressure homogenizer [25]. The physical and chemical properties of SLNs are closely associated with lipid compositions, surfactants and homogenization conditions (pressure, temperature, and number of cycles) [26]. It was reported that risperidone-loaded solid lipid nanoparticles were prepared with HPH method, and the following characterization and biocompatibility studies shown that the system was provided with good long-term stability and improved the bioaccessibility of drug [27].

The objective of this study was to develop SLNs for ASTA to improve stability and solubility by HPH. The preparation conditions including preparation parameters (pressure and number of cycles) and the content of solid lipid matrix were optimized. The chemical stability of ASTA in SLNs was investigated by comparing with free ASTA. Furthermore, the release behavior of ASTA-SLNs was evaluated in simulated gastric and intestinal juice systems.

2 Materials and methods

2.1 Materials

ASTA ($C_{40}H_{52}O_4$, 99%, 596.86 g/mol), glycerol monostearate (GMS), glycerol distearates (GDS), stearic acid (SA), and polysorbate 20 (Tween 20) were purchased from Sigma–Aldrich (Shanghai, China). Soybean oil was obtained from China Grain Reserves (Jiangsu, China). Pepsin and pancreatin were provided by Tokyo Chemical Industry (Tokyo, Japan). Methanol and acetonitrile for analytical HPLC were chromatographic grade and purchased from Merck (Hohenbrunn, Germany). Ultrapure water used for HPLC was produced by Q Millipore System (Millipore, Bedford, USA). Deionized water was used in other experiments.

2.2 Preparation of ASTA-SLNs

ASTA-SLNs were produced using HPH as described earlier by Wissing with some modification [28]. Internal lipid phase was prepared by adding the solid lipid matrix (SA, GMS, GDS) into soybean oil with heating and stirring at 75°C for 1 h to ensure the full dissolution of the mixture. The contents of solid lipid matrix were ranged from 0 to 15 wt%. ASTA was dissolved into the above mixed lipid phase at the level of 1 mg ASTA/1 g mixed lipid phase. For the sake of effective dissolution, all lipid phases were heated and stirred for 20 min under a nitrogen atmosphere. An aqueous phase was prepared by dispersing Tween 20 (10% w/w) into deionized water. Then the lipid phase was dispersed into the aqueous phase (1:9 w/w) at ambient temperature. ASTA coarse nanoemulsion was obtained using a high-speed blender (HENC, Shanghai, China) for 5 min at 13000 rpm, and then homogenized by high pressure homogenizer (AH-basic, Shanghai, China). The preparation parameters were as follows: pressure from 150 to 900 bar, cycles at 5 or 15. At the end, ASTA-SLNs were formed through the obtained nanoemulsion recrystallizing upon cooling down to room-temperature. ASTA-SLNs samples were stored at 4°C in dark for further research.

2.3 Characterization of ASTA-SLNs

The physical stability of ASTA-SLNs was evaluated by dynamic light scattering technique with Nano Zetasizer (Malvern, Worcestershire, UK). Average particle size (Z-average), polydispersity index (PDI) and zeta potential of ASTA-SLNs samples were measured. In case of multiple scattering effects, ASTA-SLNs were diluted (1:100 v/v) with ultrapure water prior to measurements. Experiments were performed at ambient-temperature 25°C at a measuring angle of 90° to the incident beam. PDI is used to analyze the particle size distribution with the value reported from 0 to 1, and the smaller value indicates that emulsion is uniform. Zeta

potential demonstrates the strength of repulsion between charged particles. In general, lower zeta potential absolute value shows that the colloidal system is not physically stable due to the rapid aggregation of droplets. The analyze data was averaged from each measurement of three independent experiments.

2.4 High performance liquid chromatography (HPLC) analysis of ASTA

The analytical HPLC equipment was a Shimadzu LC-15C system with two LC-15C solvent delivery units, a SPD-15C detector, a CTO-10ASVP column oven, a LC solution workstation (Shimadzu, Kyoto, Japan) and an analytical reversed phase C18 column (4.6×250 mm, 5 μm, Diamodsil^{TM}). The mobile phase solvents were (15% v/v) methanol, (82.5% v/v) acetonitrile, and (2.5% v/v) ultrapure water [29]. The flow rate was 1 mL/min. The temperature of the column was kept at 30°C. The detection wavelength was set at 476 nm with a resolution of 1.2 nm. The injection volume was 20 μL portion per sample. The calibration of peak area versus astaxanthin concentration was linear in the range of measures concentrations ($Y = 130\,000X + 23753$ in which Y is astaxanthin concentration (μg/mL) and X is the peak area, $R^2 = 0.9966$, $n = 5$)

ASTA in SLNs was analyzed by HPLC as follows: One milliliter of ASTA-SLNs sample was dissolved into the mixed organic extraction liquids which were composed of petroleum ether and acetonitrile (1:8 v/v). Then the colloidal system was destroyed by high-speed mixing, and then was centrifuged at 9000 rpm for 10 min. The oily phases on the top were solid lipid matrix and soybean oil, and the phases on the bottom were ASTA and the mixed organic extraction liquids. ASTA was taken out by syringe and measured by HPLC.

2.5 Storage stability of ASTA-SLNs

As known, storage conditions have a significant influence on the stability of colloidal system. In order to measure the storage stability of ASTA-SLNs, the samples of ASTA-SLNs were placed into sealed chambers at 4 and 25°C for 20 days, respectively. The particle size, PDI and zeta potential of ASTA were detected by a dynamic light-scattering instrument at a scheduled time. Each test was repeated in triplicates.

2.6 Stability of free ASTA and ASTA in SLNs

Comparative tests were performed to investigate the stability of free ASTA and ASTA in SLNs. Ten milliliters of ASTA-SLNs were put into tube, and an equivalent amount of free ASTA was dispersed into 10 mL acetonitrile. All samples were exposed to different conditions, such as light, heating, oxidation, acid, and alkali. At a fixed period of time, the retention amount of ASTA in sample was analyzed by Eg. (1). The retention rate of ASTA was calculated by Eq. (2).

$$\text{Retention amount (mg)} = C_{\text{ASTA}} \times V_{\text{ASTA}} \quad (1)$$

$$\text{Retention rate } \% = \frac{\text{Residual amount of ASTA(mg)}}{\text{Original amount of ASTA(mg)}} \times 100\% \quad (2)$$

The experiment was carried out in triplicate. The retention rate of ASTA was expressed as mean ± stand deviation (SD).

2.6.1 Light stability

The light stability of free ASTA and ASTA in SLNs were detected at a sustaining stable light source with 178 lux. All samples were exposed to the light for 15 days at 25°C in an incubator. At a prescribed time, the retention rates of free ASTA and ASTA in SLNs were measured by HPLC.

2.6.2 Thermal stability

The thermal stability of free ASTA and ASTA in SLNs were investigated at 40 and 60°C, respectively. All samples were heated for 12 h in the dark environment. The retention rates of free ASTA and ASTA in SLNs were measured by HPLC every 1.5 h.>

2.6.3 Chemical stability

The structure and properties of ASTA can be easily changed in acidic and alkaline fluids. The chemical stability of free ASTA and ASTA in SLNs were tested in aqueous solutions with the pH value ranging from 2 to 9. The retention rates of free ASTA and ASTA in SLNs were measured by HPLC.

2.6.4 Oxidation stability

The high antioxidant activity of ASTA is because of ketonic (C=O) and hydroxylic (OH) bonds that scavenge free radicals and quench singlet oxygen. In this experiment, the oxidation stability of free ASTA and ASTA in SLNs were detected in the H_2O_2 solution. All samples were dispersed into aqueous solutions with various amounts of H_2O_2 (0, 0.02, 0.04, 0.06, 0.08, 0.10 mmol). The comparative experiments were conducted at 25°C for 2 h and kept in dark for avoiding the decomposition of H_2O_2. The retention rates of free ASTA and ASTA in SLNs were measured by HPLC.

2.7 In vitro release studies

Dialysis method, studying drug release kinetics of nanoparticles system, was adopted in vitro release experiments.

The release studies of ASTA-SLNs employed the dialysis bag technique reported by Tikekar et al. [30], with some modification. Dialysis bag which was soaked overnight having a pore size of 12 Da (Sigma–Aldrich Co., Madrid, Spain) was used for this study.

2.7.1 Simulated gastric digestion

Simulated gastric fluid (SGF) was prepared as follows: Sodium chloride (5 g) was added into 1 L of deionized water, and the pH of solution was adjusted to 1.2 with 1 M HCL solution [31]. A total of 1 mL of SGF (with 0.01 g pepsin or without) was dissolved into 9 mL of ASTA-SLNs dispersion. And then 10 mL of digestion mixtures were placed in dialysis bag. The dialysis bag was placed in 1 L SGF, and incubated (37 ± 0.5°C, 100 rpm) for 2 h in thermostatic water bath oscillator. At the determined time, ASTA-SLNs sample (200 μL) was taken out and the concentration of ASTA in SLNs was analyzed by HPLC.

2.7.2 Simulated intestinal digestion

Simulated intestinal fluid (SIF) was prepared with phosphate buffer solution (pH = 6.8). A total of 1 mL of SIF (with 0.01 g pancreatin or without) was dissolved into 9 mL of ASTA-SLNs dispersion. The digestion mixtures were placed into dialysis bag and incubated (37 ± 0.5°C, 100 rpm) for 4 h in 1 L SIF as well. ASTA-SLNs sample (200 μL) was taken out and the concentration of ASTA in SLNs was measured every 30 min.

2.8 Statistical analysis

Results are expressed as mean ± standard deviation (SD). All experiments were performed in triplicate. Differences between means were considered significant when $p < 0.05$. Results were analyzed with the SPSS program (SPSS, version 12.0 for Windows, SPSS Inc.).

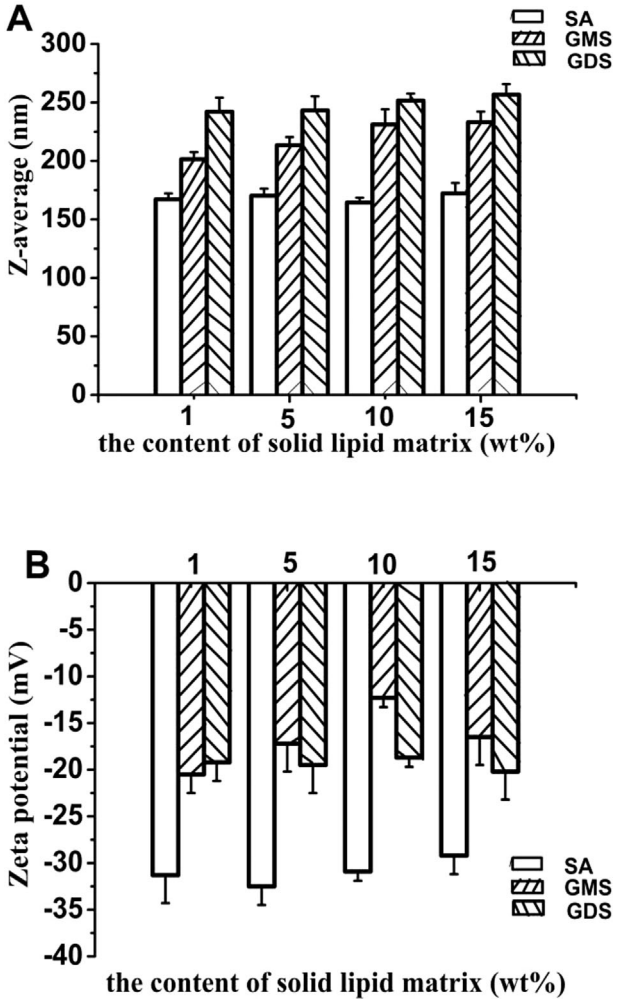

Figure 1. The physical characterization of ASTA-SLNs with SA, GMS and GDS: (A) average particle size (Z-average) of ASTA-SLNs, (B) zeta potential of ASTA-SLNs. The content of the solid lipid matrix (SA, GMS, GDS) were set at 1, 5, 10, and 15 wt%, respectively. The experiment was carried out in triplicate. The data was expressed as mean ± stand deviation (SD).

3 Results and discussion

3.1 Screening of solid lipid matrix

Lipid nucleation, made from solid lipid matrix and vegetable oil, combined with external water phase to construct SLNs. SA, GMS, and GDS, with the properties of biodegradability and low toxicity, are frequently used as solid lipid matrix for SLNs. The solid lipid matrix plays an important role in a physically stable colloidal system.

The particle size and zeta potential of ASTA-SLNs with SA, GMS, and GDS were measured, respectively. As is shown in Fig. 1A, the average particle sizes of ASTA-SLNs with different contents of SA were around 170 nm, distinctly lower than that of ASTA-SLNs with GMS and GDS. The molecular weight of SA, GMS and GDS are 284.48, 358.56, and 625.04, respectively. It was found that nanoparticle size increased along with the molecular weight of solid lipid matrix. It could be speculated that the higher molecular weight of GMS and GDS given rise to the increase of particles size.

The zeta potentials of ASTA-SLNs were shown in Fig. 1B. In general, dispersion with zeta potential values more than +20 or less than −20 mV is physically stable [32]. The zeta potential absolute values of ASTA-SLNs with GMS and GDS were under 20 mV, indicating that both of systems were not physically stable. On the contrary, all of zeta potentials of ASTA-SLNs with SA were less than −30 mV.

Tween 20, a non-ionic surfactant, had no impact on the zeta potential of SLNs. Therefore, the zeta potential of SLNs was more likely to originate from dissociation of SA either in the aqueous dispersion medium or from the particle surface [21]. In addition, with the increasing content of SA from 1 to 15 wt %, there were slight augments in particle size and zeta potential.

The solubility of drug in SLNs with single solid lipid matrix used as lipid carrier material is reduced, and the stability of SLNs with single vegetable oil used as carrier material is decreased as well [20, 33]. Therefore, mixed lipid materials including solid lipid matrix and vegetable oil have attracted increasing attention in SLNs researches. Solid lipid matrix forms fibrous crystalline networks by molecular self-assembly through noncovalent interactions in cooling progress [34]. These fibrous crystalline networks not only prevent the random movement of liquid vegetable oil, but also govern nucleation in lipid carrier of solid lipid nanoparticles [35]. In general, high molecular weight of solid lipid matrix leads to large particle size and PDI of nanoparticles [36]. As a consequence, in contrast to GDS and GMS, lower molecular weight SA yield a more compact crystalline network for decreasing the particle size of ASTA-SLNs. Additionally, it was known that high viscosity of solid lipid matrix was bad for SLNs obtaining small particle size in high pressure homogenization process [37]. The small particle size and PDI of ASTA-SLNs are just based on the low viscosity of SA. The zeta potential value is crucial to evaluate stability of SLNs. The Hydrophile–Lipophile Balance (HLB) of SA, GDS, and GMS are 15, 3.8, 2.5∼3, respectively. GDS and GMS, W/O non-ionic surfactant, were stable without ionization in water solution [38]. The ionization of hydrophilic carboxyl from SA provided more negative charge for nanoparticles, thus increasing electric repulsion between nanoparticles to avoid aggregation [39]. Furthermore, hydrophilic carboxyl could also increase water dispersion of ASTA-SLNs in aqueous solution. Consequently, ASTA-SLNs with SA were shown more physical stability than GMS and GDS in experiments.

3.2 Optimization of homogenization conditions

HPH is an appropriate method for preparing SLNs. Table 1 shows the mean particle size expressed as average particle size (Z-average), PDI and zeta potential of ASTA-SLNs for HPH technology. With the increasing of pressure, the mean particle size of ASTA-SLNs decreased from 295.4 ± 18.9 to 78.7 ± 9.6 nm. When homogenization pressures were 150 and 900 bar, all of the zeta potentials of ASTA-SLNs were higher than -30 mV. In comparison, 300 bar was fit to prepare SLNs for ASTA, with smaller particle size (167.2 ± 18.1 nm) and lower zeta potential (-36.2 ± 2.6 mV). In addition, homogenization cycles had a synergistic action on the characterization of ASTA-SLNs with the pressure. Nanoparticles had a smaller particle size under 15 cycles than that of 5 cycles condition. As a consequence, ASTA-SLNs were produced under the optimized homogenization conditions (300 bar, 15 cycles) for further research.

3.3 Storage stability of ASTA-SLNs

The changes of nanoparticle sizes with different contents of SA over time were given in Fig. 2. At 4°C, the particle size of ASTA-SLNs with 1 wt% SA content changed from 162.8 ± 7.8 to 167 ± 5.6 nm. It was easy for nanoparticles to aggregate in solution, when the content of SA was over 5 wt %. In comparison with 4°C, the data was slightly higher at 25°C. It is likely that high temperature provides more kinetic energy to accelerate the collision of particles [40]. This result indicated that ASTA-SLNs with no or lower SA content (1 wt%) had better storage stability at low temperature.

3.4 Comparing stability of free ASTA with ASTA in SLNs

With the purpose to detect the stability of free ASTA and encapsulated ASTA, comparative tests were performed in this part. As shown in Fig. 3, the effects of light on the degradation of free ASTA and ASTA in SLNs were studied. After 15 days, the retention rate of free ASTA decreased rapidly to $68.3 \pm 1.5\%$ (Fig. 3A), whereas ASTA in SLNs was slightly decomposed with less than 10% (Fig. 3B). The results indicated that SLNs were able to protect ASTA from light. When the content of SA was 1 wt%, the retention rate of ASTA in SLNs was greater than 96%. ASTA in SLNs had a degradation of 8% by increasing the content of SA to 15 wt %. This indicated that excessive content of SA was not favorable for improving the stability of ASTA. And the results were in agreement with the storage stability of ASTA-SLNs.

The thermal stability of free ASTA and ASTA in SLNs were studied at 40 and 60°C within 12 h (Fig. 4). The retention rate of free ASTA decreased rapidly to 89.2 ± 2.2 and $76.2 \pm 2.1\%$ when ASTA was heated at 40 and 60°C, respectively (Fig. 4A). The loss rate of ASTA in SLNs was less than 10% at 40°C (Fig. 4B) and 20% at 60°C (Fig. 4C). The physical stability of ASTA-SLNs suffered a challenge under heating for a long time. Because of its complex structure, ASTA was degraded into many products by multiple fracture patterns under heating [41]. With the increasing of temperature, the degradation rate of ASTA was accelerated dramatically [14]. Moreover, the aggregation of nanoparticles was also account for the loss of ASTA. However, the thermal stability of ASTA was improved through SLNs.

The chemical stability of free ASTA and ASTA in SLNs were studied in several aqueous solutions with different pH values (Fig. 5). ASTA would be inactive because of isomerization in strong acid and alkali liquids [42]. The retention rates of free ASTA were less than 60% when the pH value was 2, 3, 8, and 9 (Fig. 5A). At the same time, the

Table 1. Physicochemical characteristics (average particle size (Z-average), polydispersity index(PDI) and zeta potential) of ASTA-SLNs through HPH.

Pressure (bar)	Number of cycles	Content of SA (wt%)	Z-average (nm)	PDI	Zeta potential (mV)
150	5	0	237.4 ± 12.6	0.242 ± 0.008	−25.4 ± 3.1
		1	254.6 ± 13.7	0.271 ± 0.023	−26.2 ± 2.5
		5	216.7 ± 13.3	0.24 ± 0.025	−25.1 ± 1.4
		10	267.5 ± 14.5	0.403 ± 0.039	−23.1 ± 3.2
		15	295.4 ± 18.9	0.44 ± 0.041	−20.5 ± 1.8
	15	0	233.2 ± 15.2	0.253 ± 0.028	−26.9 ± 4.2
		1	225.3 ± 11.2	0.241 ± 0.017	−27.4 ± 1.8
		5	230.2 ± 9.8	0.234 ± 0.022	−27.3 ± 2.2
		10	241.5 ± 15.3	0.245 ± 0.045	−28.2 ± 3.4
		15	250.4 ± 15.2	0.244 ± 0.038	−25.1 ± 4.7
300	5	0	174.6 ± 16.9	0.238 ± 0.032	−30.2 ± 2.9
		1	170.3 ± 12.7	0.19 ± 0.041	−31.5 ± 3.1
		5	175.5 ± 12.8	0.226 ± 0.019	−32.1 ± 2.7
		10	177.6 ± 14.4	0.218 ± 0.03	−32.1 ± 3.5
		15	183.1 ± 15.1	0.286 ± 0.032	−30.1 ± 3.7
	15	0	163.9 ± 16.9	0.201 ± 0.018	−35.2 ± 2.8
		1	167.2 ± 18.1	0.19 ± 0.042	−36.2 ± 2.6
		5	170.3 ± 17.5	0.183 ± 0.051	−36.1 ± 2.4
		10	172.5 ± 16.6	0.142 ± 0.071	−37.7 ± 3.6
		15	173.2 ± 9.2	0.187 ± 0.031	−33.5 ± 3.8
500	5	0	147.3 ± 10.2	0.172 ± 0.019	−34.2 ± 3.9
		1	144.9 ± 13.5	0.178 ± 0.027	−32.8 ± 3.9
		5	150.3 ± 12.1	0.192 ± 0.027	−34.2 ± 3.7
		10	144.9 ± 12.1	0.231 ± 0.033	−33.1 ± 4.2
		15	147.6 ± 10.2	0.19 ± 0.031	−35.1 ± 2.8
	15	0	135.9 ± 9.2	0.21 ± 0.019	−30.2 ± 2.9
		1	135.6 ± 10.1	0.228 ± 0.042	−29.5 ± 3.5
		5	125.3 ± 11.2	0.177 ± 0.039	−29.3 ± 3.7
		10	126.8 ± 13.5	0.242 ± 0.018	−28.1 ± 3.9
		15	145.7 ± 14.9	0.253 ± 0.018	−29.2 ± 2.9
900	5	0	107.8 ± 15.7	0.156 ± 0.032	−26.3 ± 4.5
		1	104.5 ± 13.8	0.217 ± 0.037	−25.3 ± 4.3
		5	105.5 ± 12.9	0.236 ± 0.015	−24.2 ± 2.8
		10	101.5 ± 11.8	0.272 ± 0.034	−23.1 ± 2.9
		15	103.2 ± 10.8	0.245 ± 0.042	−22.3 ± 3.1
	15	0	88.8 ± 12.1	0.24 ± 0.041	−27.3 ± 2.2
		1	88.6 ± 14.2	0.31 ± 0.057	−25.2 ± 1.8
		5	83.6 ± 15.1	0.253 ± 0.063	−25.1 ± 2.7
		10	86.7 ± 9.0	0.368 ± 0.058	−24.3 ± 3.5
		15	78.7 ± 9.6	0.229 ± 0.064	−22.9 ± 4.2

retention rates of encapsulated ASTA were all greater than 60% (Fig. 5B). In particular, when the content of SA was 1 wt %, SLNs provided a more powerful protection for ASTA against isomerization. Therefore, the results indicated that the chemical stability of ASTA in SLNs was greatly increased.

The oxidation stability of ASTA was investigated in H_2O_2 aqueous solution. H_2O_2, with a strong oxidability, is often used as dispersion medium to detect the oxidation stability of encapsulated ingredients [43]. The retention rates of free ASTA and ASTA in SLNs along with the amounts of H_2O_2 are presented in Fig. 6. The retention rate of free ASTA had a sharp decline of 40.7 ± 1.9% by the increasing amount of H_2O_2 (Fig. 6A). The retention rates of ASTA in SLNs were over 70% during experiments (Fig. 6B). Especially, when the content SA was 1 wt%, the retention rate of ASTA in SLNs could reach 85.6 ± 1.2%.

Based on the above experiments, it could be concluded that the stability of ASTA was enhanced through this encapsulation technology. Conventional ASTA nanoemulsion (without solid lipid matrix) protected ASTA from degradation induced by external environment [44].

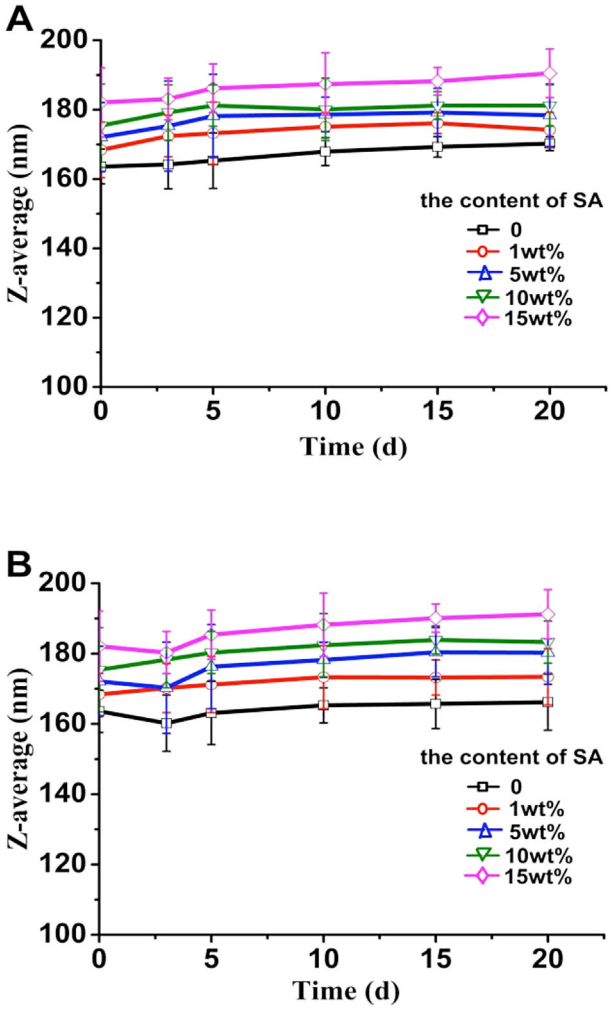

Figure 2. The storage stability of ASTA-SLNs at 4°C (A) and 25°C (B) for 20 days. The experiment was carried out in triplicate. The data was expressed as mean ± stand deviation (SD).

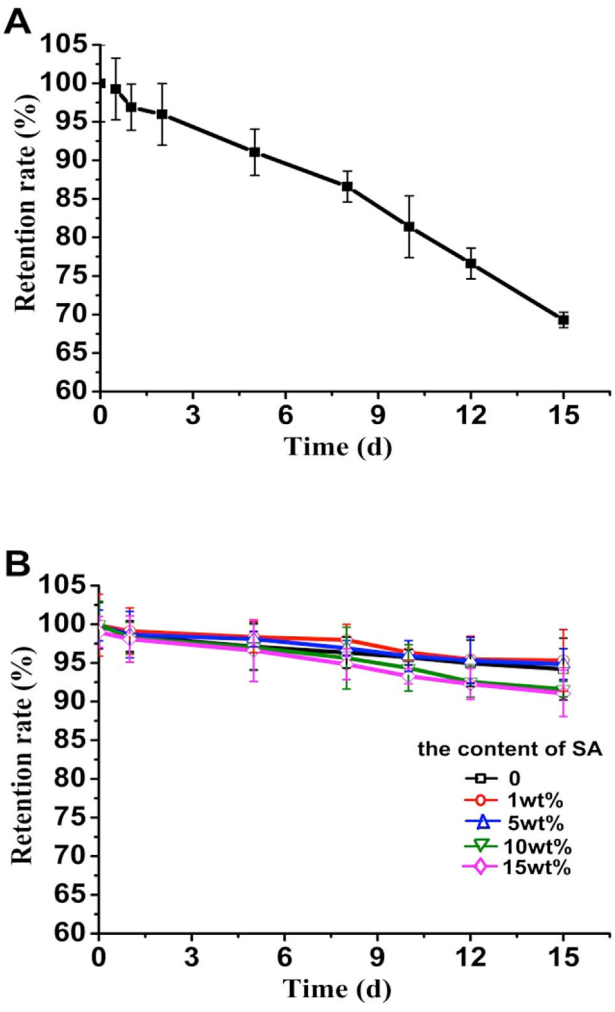

Figure 3. The light stability of free ASTA (A) and ASTA in SLNs (B). The experiment was carried out in triplicate. The data was expressed as mean ± stand deviation (SD).

Nevertheless, experimental data indicated that SLNs system could provide a more powerful protection for ASTA than nanoemulsion system. It was mainly due to that ASTA was embedded in lipid nucleation through recrystallization of SA in the refrigeration progress [45]. The optimized content of SA was 1 wt% on the basis of maximum retention rate in the studies of chemical stability.

3.5 In vitro release studies

In vitro release studies of ASTA-SLNs were performed in simulated gastrointestinal fluids. The cumulative release of ASTA from SLNs as a function of time was shown (Fig. 7). In simulated gastrointestinal fluids without pepsin, the accumulative release rate of ASTA from SLNs with 1 wt% SA content was 50.2 ± 1.5%, lower than that without SA. At the presence of pepsin, the accumulative release rate of ASTA from SLNs without SA was 51.2 ± 0.7% (Fig. 7A). These results were higher than that of astaxanthin–calcium alginate gel (ASX-CAG) beads reported by Lee et al. [46]. This may be because of that the surface structure of SLNs was damaged by strong acid, thus inducing that more ASTA was diffused into simulated gastrointestinal fluids. In acid solution (pH 1.2), the negative zeta potential of ASTA-SLNs was at 0 ~ −15 mV [39]. Hence, nanoparticles were likely to come into aggregations in acid solution, which results in the damage of surface structure [37, 47].

Release of ASTA from SLNs in simulated intestinal fluids had been investigated within 4 h (Fig. 7B). At the presence of pancreatin, the accumulative release rate of ASTA from SLNs without SA could up to 37.2 ± 3.1%, higher than 34.9 ± 1.2% of encapsulated ASTA released from SLNs with

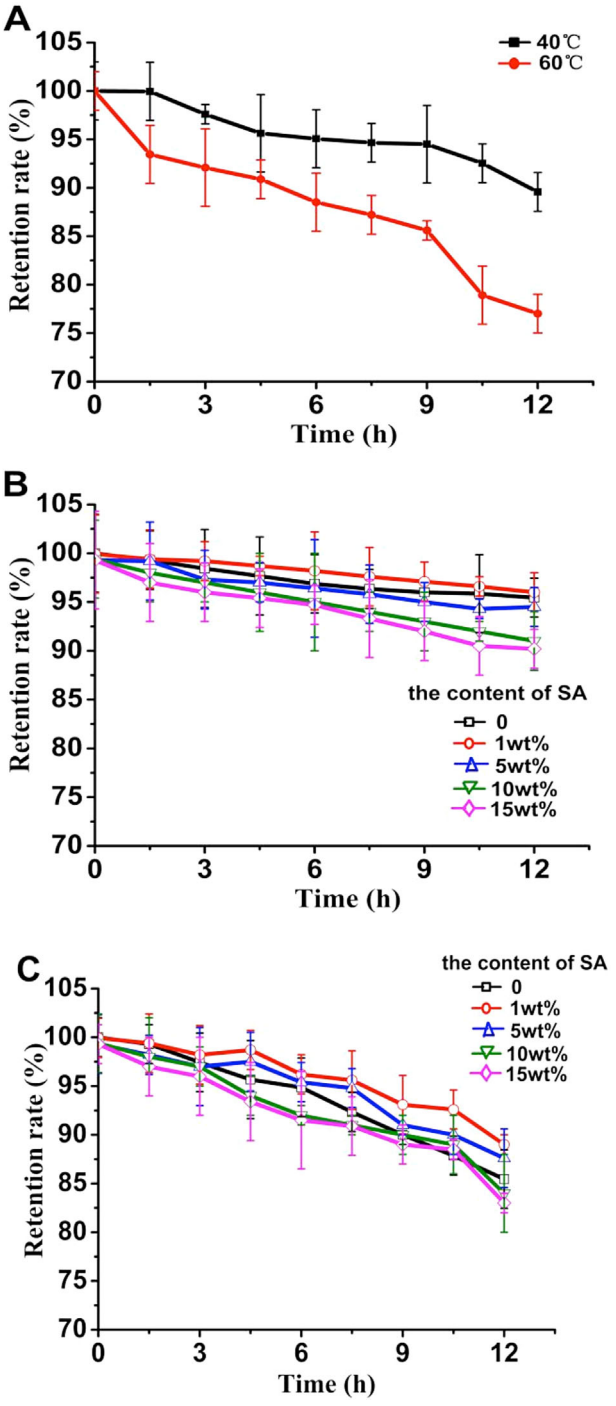

Figure 4. The thermal stability of free ASTA and ASTA in SLNs: (A) free ASTA at 40 and 60°C, (B) ASTA in SLNs at 40°C, (C) ASTA in SLNs at 60°C. The experiment was carried out in triplicate. The data was expressed as mean ± stand deviation (SD).

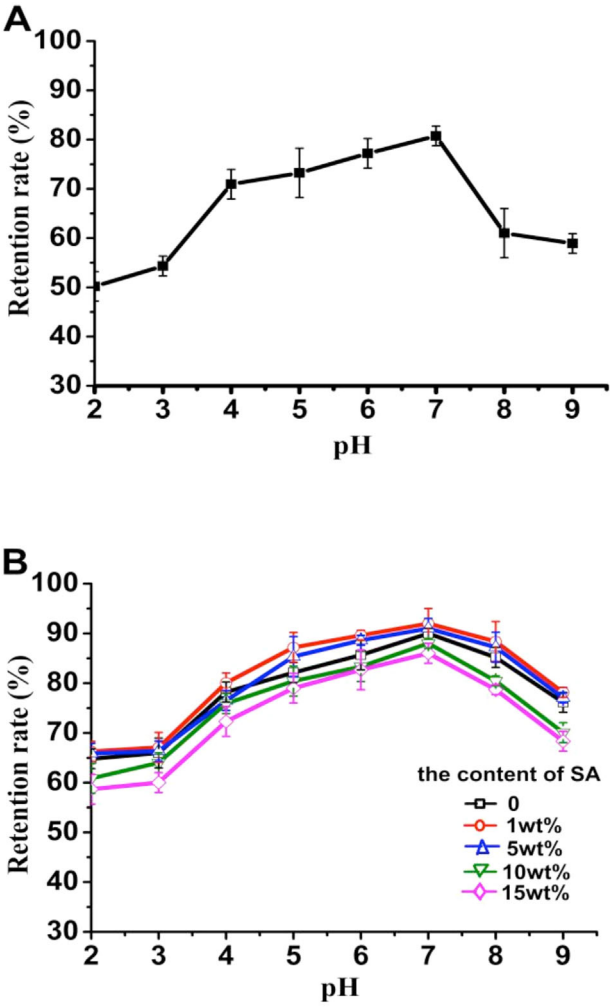

Figure 5. The effects of pH on the stabilty of free ASTA (A) and ASTA in SLNs (B). The experiment was carried out in triplicate. The data was expressed as mean ± stand deviation (SD).

1 wt% SA content. Without the presence of pancreatin, the accumulative release rate of ASTA from SLNs with 1 wt% SA content could reach only 27.5 ± 2.1%. The results demonstrated that pancreatin accelerated the diffusion rate of ASTA from lipid nucleation into simulated intestinal fluids. The release profiles of ASTA-SLNs were in agreement with the findings reported [46]. Therefore, SA could prevent ASTA against release from SLNs into simulated gastrointestinal fluids. The bioavailability of ASTA would be enhanced by its incorporation into SLNs [48].

The release behavior of ASTA depends on the structure of solid lipid nanoparticles. When single solid lipid matrix was used as carrier material, the solution ability of drug was limited by the highly ordered lattice of solid lipid matrix [49]. Soybean oil broke the lattice orientation of SA in recrystallization by inserting the lattice. Mixed lipids were beneficial to improve the encapsulation efficiency of drug by reducing crystallinity [50, 51]. Moreover, soybean oil had a good solution for liposoluble ASTA [52]. In simulated intestinal

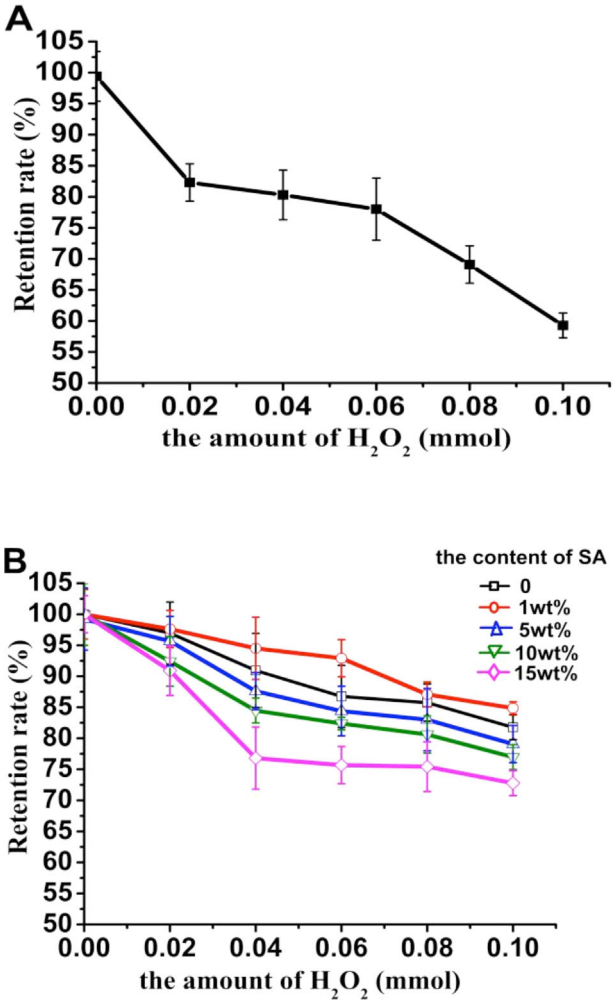

Figure 6. The oxidation stability of free ASTA (A) and ASTA in SLNs (B) in aqueous solution with various amount H_2O_2. The experiment was carried out in triplicate. The data was expressed as mean ± stand deviation (SD).

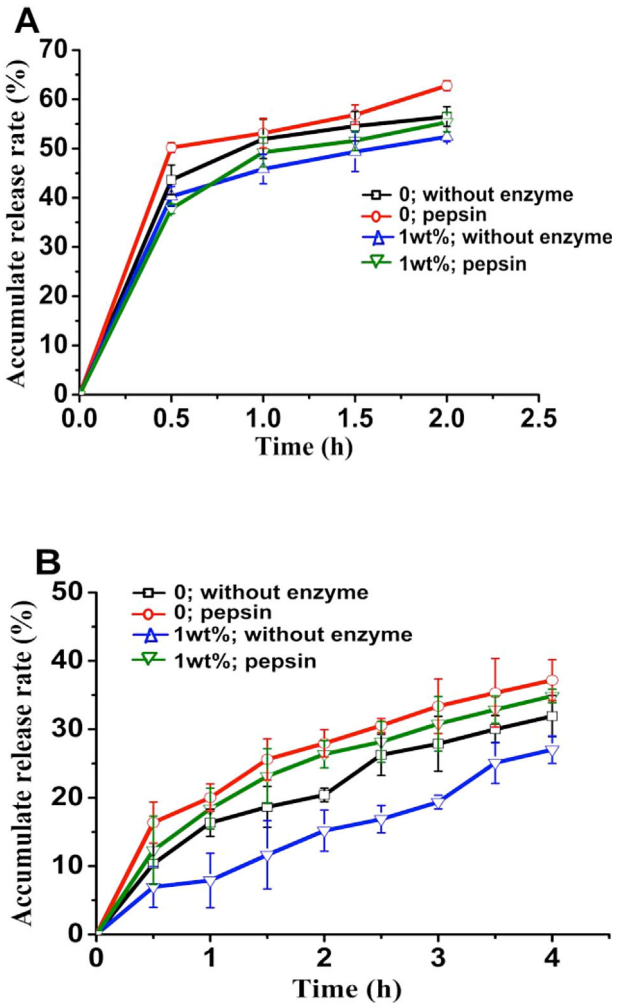

Figure 7. The cumulative release of ASTA from SLNs in simulated gastric fluid (A) and simulated intestinal fluid (B), with digestive enzymes or without. All measurements are average of three measurements. A different letter on top of the data-point represents a statistically significant difference compared to the previous value ($p < 0.05$).

fluids, pancreatin broke soybean oil into glycerol and fatty acids, thus more ASTA exposing into the solution.

4 Conclusions

In the present study, ASTA-SLNs, using SA as a solid lipid matrix and Tween 20 as an emulsifier, were prepared by HPH. ASTA-SLNs with 1 wt% SA content had good physical stability (Z-average: 167.2 ± 18.1 nm, PDI: 0.19 ± 0.042, zeta potential: −36.2 ± 2.6 mV). The optimized homogenization conditions (300 bar, 15 cycles) were needed for a more physical stable colloidal system. In addition, compared with free ASTA, the stability of ASTA in SLNs was greatly enhanced. The results indicated that SLNs afforded protection for ASTA against degradation, especially when the content of SA was 1 wt%. The release experiments of ASTA-SLNs revealed that SLNs could provide prolonged release of ASTA in simulated gastrointestinal juices. Therefore, SLNs are a promising carrier for improving the stability of ASTA.

The authors acknowledge financial support from the National High Technology Research and Development Program of China (863 Program, grant nos. 2012AA021403 and 2014AA021705), the Beijing Higher Education Young Elite Teacher Project (YETP0520), the Fundamental Research Funds for the Central Universities (YS1407), and China Scholarship Council.

The authors have declared no conflict of interest.

References

[1] Toasa, S., Cakli, S., Ostermeyer, U., Determination of astaxanthin and canthaxanthin in salmonid. *Eur. Food Res. Technol.* 2005, *221*, 787–791.

[2] Wang, L. Z., Yang, B., Yan, B. L., Yao, X. C., Supercritical fluid extraction of astaxanthin from Haematococcus pluvialis and its antioxidant potential in sunflower oil. *Innov. Food Sci. Emerg. Technol.* 2012, *13*, 120–127.

[3] Ohno, M., Darwish, W. S., Ikenaka, Y., Miki, W., et al. Astaxanthin can alter CYP1A-dependent activities via two different mechanisms: Induction of protein expression and inhibition of NADPH P450 reductase dependent electron transfer. *Food Chem. Toxicol.* 2011, *49*, 1285–1291.

[4] Preuss, H. G., Echard, B., Bagchi, D., Perricone, N. V., et al. Astaxanthin lowers blood pressure and lessens the activity of the renin-angiotensin system in zucker fatty rats. *J. Funct. Foods* 2009, *1*, 13–22.

[5] Sasski, Y., Kobara, N., Higashino, S., Giddings, J. C., et al. Astaxanthin inhibits thrombosis in cerebral vessels of stroke-prone spontaneously hypertensive rats. *Nutr. Res.* 2011, *31*, 784–789.

[6] Bhatt, P. C., Ahmad, M., Panda, B. P., Enhanced bioaccumulation of astaxanthin in Phaffia rhodozyma by utilising low-cost argo products as fermentation substrate. *Biocatal. Agric. Biotechnol.* 2013, *2*, 58–63.

[7] Yuan, C., Du, L., Jin, Z. Y., Xu, X. M., Storage stability and antioxidant activity of complex of astaxanthin with hydroxypropyl-β-cyclodextrin. *Carbohydr. Polym.* 2013, *91*, 385–389.

[8] Park, S. A., Ahn, J. B., Choi, S. H., Lee, L. S., et al. The effect of particle size on the physicochemical properties of optimized astaxanthin-rich xanthophyllomyces dendrorhous-loaded micropaticles. *LWT-Food Sci. Technol.* 2014, *55*, 638–644.

[9] Pu, J. N., Bankston, J. D., Sathivel, S., Developing microencapsulated flaxseed oil containing shrimp (Litppenaeus setiferus) astaxanthin using a pilot scale spray dryer. *Biosyst. Eng.* 2011, *108*, 121–132.

[10] Augustin, M. A., Abeywardena, M. Y., Patten, G., Head, R., et al. Effects of microencapsulation on the gastrointestinal transit and tissue distribution of a bioactive mixture of fish oil tributurin and resveratrol. *J. Food Eng.* 2011, *3*, 25–37.

[11] Wang, G. Y., Chen, J., Shi, Y. P., Preparation of microencapsulated xanthophyll for improving solubility and stability by nanoencapsulation. *J. Food Eng.* 2013, *117*, 82–88.

[12] Yuan, C., Jin, Z. Y., Xu, X. M., Inclusion complex of astaxanthin with hydroxypropyl-β-cyclodextrin: UV, FTIR, 1HNMR and molecular modeling studies. *Carbohydr. Polym.* 2012, *89*, 492–496.

[13] Yuan, C., Jin, Z. Y., Xu, X. M., Zhuang, H. N., et al. Preparation and stability of the inclusion complex of astaxanthin with hydroxypropyl-β-cyclodextrin. *Food Chem.* 2008, *109*, 264–268.

[14] Tachaprutinun, A., Udomsup, T., Luadthong, C., Wanichwecharung, S., Preventing the thermal degradation of astaxanthin through nanocapsulation. *Int. J. Pharm.* 2009, *374*, 119–124.

[15] Rostami, E., Kashanian, S., Azandaryani, A. H., Faramarzi, H. M., Dolatabadi, J. E. N., et al. Drug targeting using solid lipid nanoparticles. *J. Chem. Phys. Lett.* 2014, *181*, 56–61.

[16] Kuo, Y. C., Chen, H. H., Entrapment and release of saquinavir using novel cationic solid lipid nanoparticles. *Int. J. Pharm.* 2009, *365*, 206–213.

[17] Kheradmandnia, S., Vasheghani-Farahani, E., Nosrati, M., Atyabi, F., Preparation and characterizaiton of keptoprofen-loaded solid lipid nanoparticles made from beeswax and carnauba wax. *Nanomedicine* 2010, *6*, 753–759.

[18] Lee, M. K., Lim, S. J., Kim, C. K., Preparation, characterization and in vitro cytotoxicity of paclitaxel-loaded sterically stabilized solid lipid nanoparticles. *Biomaterials* 2007, *28*, 2137–2146.

[19] Mehnert, W., Karsten, M., Solid lipid nanoparticles: Production, characterization and application. *Adv. Drug Deliv. Rev.* 2012, *64*, 83–101.

[20] Blasi, P., Giovagnoli, S., Schoubben, A., Ricci, M., et al. Solid lipid nanoparticles for targeted brain drug delivery. *Adv. Drug Deliv. Rev.* 2007, *59*, 454–477.

[21] Shah, R. M., Malherbe, F., Eldridge, D., Palombo, E. A., et al. Physicochemical characterization of solid lipid nanoparticles (SLNs) prepared by a novel microemulsion technique. *J. Colloid Interface Sci.* 2014, *428*, 286–294.

[22] Almeida, A. J., Souto, E., Solid lipid nanoparticles as a drug delivery system for pepties ans proteins. *Adv. Drug Deliv. Rev.* 2007, *59*, 478–490.

[23] Gastaldi, L., Battaglia, L., Peira, E., Chirio, D., et al. Solid lipid nanoparticles as vehicles of drugs to the brain: Current state of the art. *Eur. J. Pharm. Biopharm.* 2014, *87*, 433–444.

[24] Luo, Y. C., Teng, Z., Li, Y., Wang, Q., Solid lipid nanoparticles for oral drug delivery: Chitosan coating improves stability, controlled delivery, mucoadhesion and cellular uptake. *Carbohydr. Polym.* 2015, *122*, 221–229.

[25] Jin, S. G., Zhang, G. M., Zhang, P. Y., Fan, S. Y., et al. High-pressure homogenization pretreatment of four different lignocellulosic biomass for enhancing enzymatic disgestibility. *Bioresour. Technol.* 2015, *181*, 270–274.

[26] Martins, S., Tho, I., Reimold, I., Fricher, G., et al. Brain delivery of camptothecin by means of solid lipid nanoparticles: Formulation design, in vitro and in vivo studies. *Int. J. Pharm.* 2012, *439*, 49–62.

[27] Silva, A. C., González-Mira, E., García, M. L., Egea, M. A., et al. Preparation, characterization and biocompatility studies on risperidone-loaded solid lipid nanoparticles (SLN): High pressure homogenization versus ultrasound. *Colloids Surf. B* 2011, *86*, 158–165.

[28] Wissing, S. A., Kayser, O., Muller, R. H., Solid lipid nanoparticles for parenteral drug delivery. *Adv. Drug Deliv. Rev.* 2004, *56*, 1257–1272.

[29] Anarjan, N., Tan, C. P., Nehdi, I. A., Ling, T. C., Colloidal astaxanthin: Preparation, characterisation and bioavailability evaluation. *Food Chem.* 2012, *135*, 1303–1309.

[30] Tikekar, R. V., Pan, Y. J., Nitin, N., Fate of curcumin encapsulated in silica nanoparticles stabilized pickering emulsion during storage and simulated digestion. *Food Res. Int.* 2013, *51*, 370–377.

[31] Sarkar, A., Horne, D. S., Singh, H., Interactions of milk protein-stabilized oil-in-water emulsions with bile salts in a simulated upper intestinal model. *Food Hydroch.* 2010, *24*, 142–151.

[32] Das, S., Ng, W. K., Tan, R. B. H., Are nanostructured lipid carriers (NLCs) better than solid lipid nanoparticles (SLNs): Development, characterizations and comparative

evaluations of clotrimazole-loaded SLNs and NLCs? *Eur. J. Pharm. Sci.* 2012, *47*, 139–151.

[33] Kumar, S., Randhawa, J. K., High melting lipid based approach for drug delivery: Solid lipid nanoparticles. *Mater. Sci. Eng. C* 2013, *33*, 1842–1852.

[34] Sagiri, S. S., Singh, V. K., Pal, K., Banerjee, I., et al. Stearic acid based oleogels: A study on the molecular, thermal and mechanical properties. *Mater. Sci. Eng. C* 2015, *48*, 688–699.

[35] Severino, P., Pinho, S. C., Souto, E. B., Santana, M. H. A., Polymorphism, crystallinity and hydrophilic-lipophilic balance of stearic acid and stearic acid-capric/caprylic triglyceride matrices for production of stable nanoparticles. *Colloids Surf. B* 2011, *86*, 125–130.

[36] Xie, S. Y., Zhu, L. Y., Dong, Z., Wang, X. F., et al. Preparation, characterization and pharmacokinetics of enrofloxacin-loaded solid nanoparticles: Influence of fatty acids. *Colloids Surf. B* 2011, *83*, 382–387.

[37] Hu, F. Q., Jiang, S. P., Du, Y. Z., Yuan, H., et al. Preparation and characterization of stearic acid nanostructured lipid carrier by solvent diffusion method in an aqueous system. *Colloids Surf. B* 2005, *45*, 167–173.

[38] Fanun, M., Properties of microemulsions based on mixed nonionic surfactants and mixed oils. *J. Mol. Liq.* 2009, *150*, 25–32.

[39] Usui, S., Healy, T. W., Zeta potential of stearic acid monolayer at the air-aqueous solution interface. *J. Colloid Interface Sci.* 2002, *250*, 371–378.

[40] Yuan, H., Chen, J., Du, Y. Z., Hu, F. Q., et al. Studies on oral absorption of stearic acid SLN by a novel fluorometric method. *Colloids Surf. B* 2007, *58*, 157–164.

[41] Yuan, C., Jin, Z. Y., Thermal stability and decomposition kinetic of astaxanthin. *Nat. Prod. Res. Dev.* 2010, *22*, 1085–1087.

[42] Aanrjan, N., Tan, C. P., Chemical stability of astaxanthin nanodispersions in organge juice and skimmed milk as model food systems. *Food Chem.* 2013, *139*, 527–731.

[43] Wu, H. H., Liang, H., Yuan, Q. P., Wang, T. X., et al. Preparation and stability investigation of the inclusion complex of sulforaphane with hydroxypropyl-β-cylcodextrin. *Carbohydr. Polym.* 2010, *82*, 613–617.

[44] Qian, C., Decker, E. A., Xiao, H., McClements, D. J., Inhibition of β-carotene degradation in oil-in-water nanoemulsions: Influence of oil-soluble and water-soluble antioxidants. *Food Chem.* 2012, *135*, 1036–1043.

[45] Jasch, K., Barth, N., Fehr, S., Bunjes, H., et al. A microfluidic approach for a continuous crystallization of drug carrier nanoparticles. *Chem. Eng. Technol.* 2009, *32*, 1806–1814.

[46] Lee, J. S., Park, S. A., Chuang, D. H., Lee, H. J., Encapsulation of astaxanthin-rich Xanthophyllomyces dendrorhous for antioxidant delivery. *Int. J. Biol. Macromol.* 2011, *49*, 268–273.

[47] Muller, R. H., Mader, K., Gohla, S., Solid lipid nanoparticles (SLN) for controlled drug delivery - a review of the state of the art. *Eur. J. Pharm. Biopharm.* 2000, *50*, 161–177.

[48] Odeberg, J. M., Lignell, Å., Pettersson, A., Höglund, P., Oral bioavailability of the antioxidant astaxanthin in humans is enhanced by incroporation of lipid based formulations. *Eur. J. Pharm. Sci.* 2003, *19*, 299–304.

[49] Jenning, V., Thunemann, A. F., Gohla, S. H., Characterization of a novel solid lipid nanoparticles carrier system based on binary mixtures of liquid and solid lipids. *Int. J. Pharm.* 2000, *199*, 167–177.

[50] Ratanapariyanuch, K., Clancy, J., Emami, S., Cutler, J., Reaney, M. J. T., Physical, chemical, and lubricant properties of Brassicaceae oil. *Eur. J. Lipid Sci. Technol.* 2013, *115*, 1005–1012.

[51] Bunjes, H., Westesen, K., Michel, H. J. Koch, Crystallization tendency and polymorphic transitions in triglyceride nanoparticles. *Int. J. Pharm.* 1996, *129*, 159–173.

[52] Lakshminarayana, R., Baskaran, V., Influence of olive oil on the bioavailability of carotenoids. *Eur. J. Lipid Sci. Technol.* 2013, *115*, 1085–1093.

